formation of a strong axial bond. In the present case the steric repulsion is also relieved by a considerable twisting (18.8°) of the bridging ligands. In $Ru_2(mhp)_4$[11] where there is no axial coordination, the molecule has a 2:2 arrangement, as expected.

Acknowledgment. We are grateful to the National Science Foundation for financial support.

Supplementary Material Available: Details of the crystal structure determination, a unit cell diagram, and tables of structure factors, anisotropic thermal parameters, and bond distances and angles (16 pages). Ordering information is given on any current masthead page.

Notes

Contribution from the Department of Chemistry,
Howard University, Washington, D.C. 20059

Kinetics of the Reduction of Manganese(III) Porphyrins by Hexaammineruthenium(II): A Reductive Acid Solvolysis Mechanism

Robert Langley and Peter Hambright*

Received June 19, 1984

The reagents ascorbic acid,[1] pentacyanocobaltate(II),[2] dithionite,[3-6] europium(II),[7] chromium(II),[7-11] tin(II),[12] and vanadium(II)[7,8] have been used to probe the mechanisms of reduction of trivalent iron, cobalt, and manganese water-soluble porphyrins to their divalent forms. In many cases, the reactions are of uncertain mechanism and with strong reductants and hydrodynamically easily reduced porphyrins, both central metal ion and ring reduction occur. The $Ru(NH_3)_6^{2+}$ ion is a well-characterized weak outer-sphere reductant, and its reactions with cobalt(III)[8,13,14] and iron(III)[15] porphyrins have been analyzed in terms of the Marcus theory[16] to provide electron-exchange rate constants for these coordinated metal ions. We report the reduction kinetics of several manganese(III) metalloporphyrins with $Ru(NH_3)_6^{2+}$. The overall mechanism involves a reductive demetalation process, and the results are compared with related electron-transfer and acid solvolysis reactions.

Experimental Section

Trifluoromethanesulfonic acid (3M Co.) was distilled under reduced pressure as the monohydrate (HTF). Lithium triflate was prepared from HTF and Li_2CO_3. Hexaammineruthenium(III) chloride (Matthey Bishop) was purified by recrystallization[17] and converted into the triflate salt[18] by precipitation of the chloride salt from distilled water using HTF. The sodium salt of manganese(III) tetrakis(4-sulfonatophenyl)porphyrin, Mn^{III}–TPPS, was prepared by literature methods.[19]

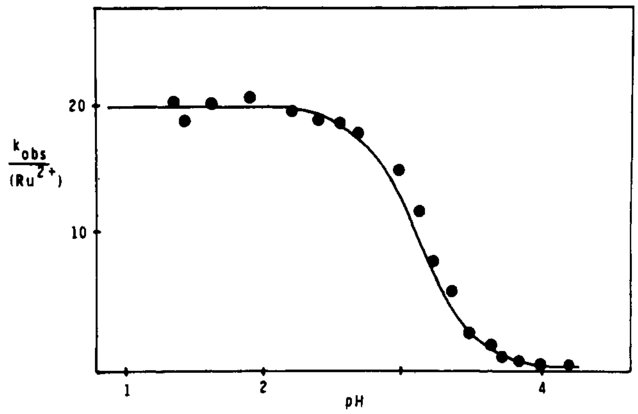

Figure 1. pH profile of the specific rates of the $Ru(NH_3)_6^{2+}$ reduction of Mn^{III}–TPPS at 25 °C and $I = 0.3$ (HTF/LiTF). The dots are experimental points, and the solid line is the theoretical curve calculated from eq 4.

All solutions were deaerated with chromous scrubbed argon. $Ru(NH_3)_6^{3+}$ was reduced to the divalent state with Zn-Hg and analyzed either by titration with permanganate[8] or spectrophotometrically by reduction of iron(III) and determination of the iron(II) formed as the tris(*o*-phenanthroline) complex.[17] The solutions were handled in Hamilton all-glass syringes with platinum needles, as stainless steel needles caused reduction of Mn^{III}–TPPS in acid.

The kinetics were followed at 25 °C on a Beckman Acta III recording spectrophotometer, or with a Durrum Gibson stopped-flow apparatus. The ionic strength (I) was maintained at 0.3 (HTF/LiTF). Chloroacetic acid (7.5×10^{-3} M) was the buffer between pH 2 and 4, while phthalic acid at the same concentration was used between pH 4 and 5. The reactions were run under pseudo-first-order conditions, with a greater than 100-fold excess of ruthenium to porphyrin (ca. 10^{-6} M). The reactions were found to be first order in Mn^{III}–P over 3 half-lives.

Results

At pH 1 ($I = 0.5$ (NaCl/HCl)), Mn^{III}–TPPS had bands at 466 nm ($\epsilon = 9.8 \times 10^4$ M^{-1} s^{-1}), 400 nm (6.1×10^4 M^{-1} s^{-1}), and 377 nm (5.9×10^4 M^{-1} s^{-1}). The compound followed Beer's law from 1×10^{-4} to 1×10^{-6} M at this pH, a result in agreement with relaxation studies[20] indicating that Mn^{III}–TPPS is monomeric in acid solution. The absorption spectra of constant concentrations of Mn^{III}–TPPS at the same ionic strength ($I = 0.2$) were carefully monitored between pH 1 and 10, and no changes were observed. Above pH 10, the Soret band decreased and broadened with further increases in pH. It appears that H_2O–Mn^{III}–TPPS does not hydrolyze below pH 10, while a variety of forms (HO–Mn^{III}–P, $(HO)_2$–Mn^{III}–P, and P–Mn^{III}–O–Mn^{III}–P) may occur in the basic region.

Between pH 1 and 4, the addition of excess $Ru(NH_3)_6^{2+}$ to Mn^{III}–TPPS produces sets of isosbestic points (the same as shown[12] in the Sn^{II}/Mn^{III}–TPPS reaction in 1 M HCl) as Mn^{III}–TPPS was transformed into the diacid H_4–$TPPS^{2-}$ metal-free porphyrin. While no evidence was found for Mn^{II}–TPPS in this pH range, it can be produced by dithionite[6,19] reduction of Mn^{III}–TPPS in base at pH 13 or by pulse radiolysis techniques.[21]

---

(1) Oxley, J. C.; Toppen, D. L. *Inorg. Chem.* **1978**, *17*, 3119
(2) Worthington, P.; Hambright, P. *Inorg. Chim. Acta* **1980**, *46*, L87.
(3) Worthington, P.; Hambright, P. *J. Inorg. Nucl. Chem.* **1980**, *42*, 1651.
(4) Pasternack, R. F.; Cobb, M. A.; Sutin, N. *Inorg. Chem.* **1975**, *14*, 866.
(5) Casset, J.; Kukuruzinsla, M.; Bender, J. *Inorg. Chem.* **1977**, *16*, 3371.
(6) Hambright, P.; Chock, P. B. *Inorg. Chem.* **1974**, *13*, 3029.
(7) Fleischer, E. B.; Hambright, P. *Inorg. Chem.* **1965**, *4*, 912.
(8) Fleischer, E. B.; Cheung, K. *J. Am. Chem. Soc.* **1976**, *98*, 8381.
(9) Reid, J.; Hambright, P. *Inorg. Chem.* **1978**, *17*, 2329.
(10) Balahura, R. J.; Trivedi, C. P. *Inorg. Chem.* **1978**, *17*, 3130.
(11) Pasternack, R. F.; Sutin, N. *Inorg. Chem.* **1974**, *13*, 1956.
(12) Hambright, P.; Williams, R. F. X. In "Porphyrin Chemistry Advances"; Longo, F. R., Ed.; Ann Arbor Science Publishers: Ann Arbor, MI, 1978; Chapter 22.
(13) Pasternack, R. F. *Inorg. Chem.* **1976**, *15*, 643.
(14) Rohrback, D. F.; Deutsch, E.; Heineman, W. R.; Pasternack, R. F. *Inorg. Chem.* **1977**, *16*, 2650.
(15) Pasternack, R. F.; Spiro, E. G. *J. Am. Chem. Soc.* **1978**, *100*, 968.
(16) Marcus, R. A. *Annu. Rev. Phys. Chem.* **1964**, *15*, 1964.
(17) Pladziewicz, J. R.; Meyer, T. J.; Broomhead, J. A.; Taube, H. *Inorg. Chem.* **1973**, *12*, 639.
(18) Lavallee, D. K., personal communication.
(19) Harriman, A.; Neta, P. *J. Phys. Chem.* **1984**, *88*, 1575.
(20) Krishnamurthy, M.; Sutter, J. R.; Hambright, P. *J. Chem. Soc., Chem. Commun.* **1975**, 13.

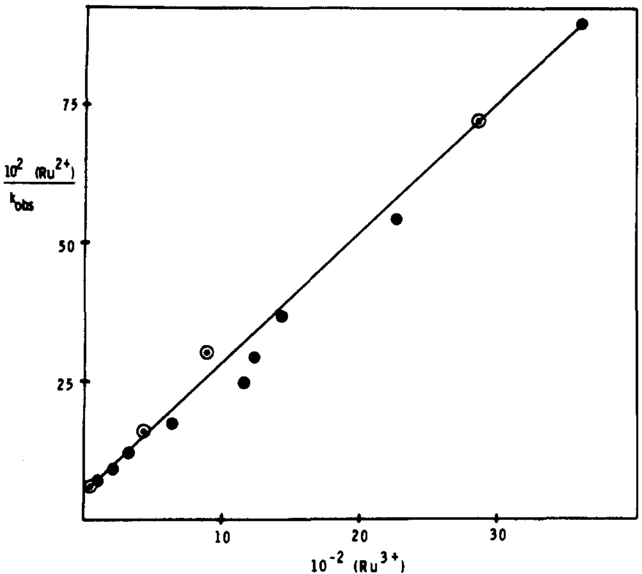

Figure 2. Plot of $[\mathrm{Ru(NH_3)_6}^{2+}]/k_{\mathrm{obsd}}$ vs. $[\mathrm{Ru(NH_3)_6}^{3+}]/[\mathrm{H}^+]^2$ according to eq 5. The dark dots are data at constant $[\mathrm{Ru(NH_3)_6}^{3+}]$ and different pHs, while the open circles are at constant pH and various $\mathrm{Ru(NH_3)_6}^{3+}$ concentrations.

In our initial experiments, $\mathrm{Ru(NH_3)_6}^{2+}$ was generated in 0.5 M HCl by reduction of the trivalent form with less than a stoichiometric amount of Eu^{2+} (from Zn–Hg reductions of Eu^{3+}). At such high acidities, the reductions were first order in $\mathrm{Mn^{III}}$–TPPS. However, at the same pH and measured ruthenium concentration, the observed rate constants increased linearly with time elapsed after ruthenium(II) formation. After 1 h, $k_{\mathrm{obsd}}/[\mathrm{Ru(NH_3)_6}^{2+}]$ was ca. 10^3 $\mathrm{M^{-1}\ s^{-1}}$, and when extrapolated back to $t = 0$, the specific rate was ≤ 50 $\mathrm{M^{-1}\ s^{-1}}$. Later experiments at higher pH values indicated that $\mathrm{Ru(NH_3)_5H_2O}$, which slowly forms under strong-acid conditions,[22] was not responsible for the dramatic specific rate increases with time at low pH. Such phenomena in acidic solutions containing ruthenium ammines may indicate a new, slowly generated, extremely reactive species, and similar behavior has been noted in acid by other workers.[23]

The system was well behaved above pH 1, when $\mathrm{Ru(NH_3)_6}^{2+}$ was generated at pH 3 by Zn–Hg reductions under argon. Between pH 1 and 2, $k_{\mathrm{obsd}}/[\mathrm{Ru(NH_3)_6}^{2+}]$ was constant (19 ± 2 $\mathrm{M^{-1}\ s^{-1}}$) in the range 2.0×10^{-3}–2.0×10^{-4} M, independent of the time at which $\mathrm{Ru(NH_3)_6}^{2+}$ was formed and independent of the amount of $\mathrm{Ru(NH_3)_6}^{3+}$ present (8×10^{-3}–1×10^{-6} M). At constant $\mathrm{Ru(NH_3)_6}^{2+}$ levels, the specific rate was independent of pH between 1 and 2 and decreased sharply with increasing pH up to pH 4 (Figure 1). At pHs between 3 and 4, $k_{\mathrm{obsd}}/[\mathrm{Ru}^{2+}]$ decreased with an increase in $\mathrm{Ru(NH_3)_6}^{3+}$ concentration, at constant ionic strength. The assumed mechanism is

$$\mathrm{Ru(NH_3)_6}^{2+} + \mathrm{Mn^{III}\text{–}P} = \mathrm{Ru(NH_3)_6}^{3+} + \mathrm{Mn^{II}\text{–}P} \quad k_1, k_{-1} \tag{1}$$

$$\mathrm{Mn^{II}\text{–}P} + 2\mathrm{H}^+ \rightarrow \mathrm{H_2\text{–}P} + \mathrm{Mn}^{2+} \quad k_2 \tag{2}$$

$$\mathrm{H_2\text{–}P} + 2\mathrm{H}^+ = \mathrm{H_4\text{–}P}^{2+} \quad \text{fast} \tag{3}$$

With $\mathrm{Mn^{II}}$–P as a steady-state intermediate, and k_2 the rate-determining step, the observed rate law in terms of the pseudo-first-order rate constant, k_{obsd}, is of the form

$$k_{\mathrm{obsd}} = k_1 k_2[\mathrm{Ru(NH_3)_6}^{2+}][\mathrm{H}^+]^2/(k_{-1}[\mathrm{Ru(NH_3)_6}^{3+}] + k_2[\mathrm{H}^+]^2) \tag{4}$$

Upon rearrangement

$$[\mathrm{Ru}^{2+}]/k_{\mathrm{obsd}} = 1/k_1 + (k_{-1}/k_1 k_2)([\mathrm{Ru}^{3+}]/[\mathrm{H}^+]^2) \tag{5}$$

Table I. Data for the $\mathrm{Ru(NH_3)_6}^{2+}/\mathrm{Mn^{III}}$–TPPS Reaction[c]

pH	$[\mathrm{Ru(NH_3)_6}^{2+}]$, M	$[\mathrm{Ru(NH_3)_6}^{3+}]$, M	$k_{\mathrm{obsd}}/[\mathrm{Ru(NH_3)_6}^{2+}]$, $\mathrm{M^{-1}\ s^{-1}}$ obsd	$k_{\mathrm{obsd}}/[\mathrm{Ru(NH_3)_6}^{2+}]$, $\mathrm{M^{-1}\ s^{-1}}$ calcd[a]
1.00[b]	3.7×10^{-4}	$\leq 10^{-6}$	21	19
1.19	2.0×10^{-3}	8.5×10^{-4}	18	19
1.43[b]	2.0×10^{-4}	$\leq 10^{-6}$	18	19
1.62	4.4×10^{-3}	8.5×10^{-4}	19	19
1.90	4.4×10^{-3}	8.5×10^{-3}	20	19
1.93	6.5×10^{-4}	1.2×10^{-4}	20	19
2.21	9.4×10^{-4}	1.2×10^{-4}	19	19
2.68	9.4×10^{-4}	1.2×10^{-3}	19	19
2.97	9.4×10^{-4}	1.2×10^{-3}	15	13
3.12	9.4×10^{-4}	1.2×10^{-3}	10	9.5
3.22	9.4×10^{-4}	1.2×10^{-3}	7.9	7.4
3.36	9.4×10^{-4}	1.2×10^{-3}	5.7	4.8
3.53	9.4×10^{-4}	1.2×10^{-3}	2.7	2.6
3.63	9.4×10^{-4}	1.2×10^{-3}	1.8	1.7
3.73	9.4×10^{-4}	1.2×10^{-3}	1.1	1.1
4.0	9.4×10^{-4}	1.2×10^{-3}	0.34	0.32
3.12	6.5×10^{-4}	2.5×10^{-4}	6.3	6.3
3.12	6.5×10^{-4}	5.0×10^{-4}	3.4	3.9
3.14	6.5×10^{-4}	1.0×10^{-3}	1.9	2.0

[a] Calculated from the parameters of eq 5. [b] Estimated amount of $\mathrm{Ru(NH_3)_6}^{3+}$ in the "pure" $\mathrm{Ru(NH_3)_6}^{2+}$ solution. [c] Conditions: 25 °C; $I = 0.3$.

Figure 2 shows the linear relationship between $[\mathrm{Ru}^{2+}]/k_{\mathrm{obsd}}$ and $[\mathrm{Ru}^{3+}]/[\mathrm{H}^+]^2$ dictated by eq 5, with $k_1 = 19 \pm 2$ $\mathrm{M^{-1}\ s^{-1}}$, and $k_{-1}/k_2 = (4.5 \pm 0.5) \times 10^{-3}$ M. Figure 1 is the pH profile of the reaction, where the solid line was calculated from the derived parameters. Table I shows representative data of the observed specific rates and those calculated according to eq 5. No chloride catalysis was found when, at constant ionic strength, LiCl was substituted for LiTF. At pH 1.5, k_1 was independent of ionic strength between $I = 0.1$ and 0.5, and at this pH, the $\mathrm{Ru(NH_3)_5H_2O}^{2+}/\mathrm{Mn^{III}}$–TPPS reaction had a specific rate of 18 $\mathrm{M^{-1}\ s^{-1}}$ (similar to the hexaammine result).

We attempted to use a palladium–asbestos catalyst[24] with $\mathrm{H_2(g)}$ to generate $\mathrm{Mn^{II}}$–TPPS at pH 5 and follow the acid solvolysis kinetics as a function of $[\mathrm{H}^+]$. However, as $\mathrm{Mn^{II}}$–TPPS formed, it was then reduced at the porphyrin ring to unidentified products. A rough estimate of $k_{\mathrm{obsd}}/[\mathrm{H}^+]^2 = 2 \times 10^8$ $\mathrm{M^{-2}\ s^{-1}}$ was made between pH 3.3 and 4.2, $I = 0.1$ (LiCl/HCl).

$\mathrm{Ru(NH_3)_6}^{2+}$ reduced manganese(III) tetrakis(*N*-methyl-4-pyridiniumyl)porphyrin ($\mathrm{Mn^{III}}$–TMPyP(4)) and its 3-isomer to essentially colorless, ring-reduced products. A brief study of the $\mathrm{Ru(NH_3)_6}^{2+}$ reaction with manganese(III) tetrakis(*N*,*N*,*N*-trimethyl-4-aniliniumyl) porphyrin ($\mathrm{Mn^{III}}$–TAP) gave results analogous to those for the TPPS system, with $k_1 = 33$ $\mathrm{M^{-1}\ s^{-1}}$ and $k_{-1}/k_2 = 5.5 \times 10^{-3}$ M.

Discussion

The rate law for the $\mathrm{Ru(NH_3)_6}^{2+}/\mathrm{Mn^{III}}$–TPPS reaction is consistent with a reductive acid solvolysis process, as shown before[25] for the $\mathrm{Fe^{III}}$–P/Fe^{2+} reactions in acetic acid. The reduction potential[26] for $\mathrm{Mn^{III/II}}$–TPPS is –0.18 V vs. NHE, and the oxidation potential for $\mathrm{Ru(NH_3)_6}^{2+/3+}$ is –0.065 V; thus the equilibrium constant K for the $\mathrm{Ru(NH_3)_6}^{2+}/\mathrm{Mn^{III}}$–TPPS reaction (eq 1) is 7.2×10^{-5}. The driving force for the overall reaction arises from the acid solvolysis step: any $\mathrm{Mn^{II}}$–TPPS formed is either oxidized to $\mathrm{Mn^{III}}$–TPPS by $\mathrm{Ru(NH_3)_6}^{3+}$ or reacts with protons in an irreversible step to form the free base $\mathrm{H_2}$–TPPS and then the observed diacid $\mathrm{H_4\text{–}TPPS}^{2-}$. At high acidity when $k_2[\mathrm{H}^+]^2 > k_{-1}[\mathrm{Ru}^{3+}]$, k_{obsd} is independent of $[\mathrm{H}^+]$ and $[\mathrm{Ru}^{3+}]$, and the reduction step k_1 (=19 $\mathrm{M^{-1}\ s^{-1}}$) is rate limiting. At high pH where

---

(21) Morehouse, K. M.; Neta, P. *J. Phys. Chem.* **1984**, *88*, 1575.

(22) Ford, P. C.; Kuempel, J. R.; Taube, H. *Inorg. Chem.* **1968**, *7*, 1976.

(23) Ford, P. C. *Coord. Chem. Rev.* **1970**, *5*, 75.

(24) Fleischer, E. B.; Ferra, R. V. *J. Inorg. Biochem.* **1979**, *10*, 91.

(25) Espenson, J.; Christensen, R. *Inorg. Chem.* **1977**, *16*, 2561.

(26) Peretz, P.; Solomon, D.; Weinraub, D.; Faraggi, M. *Int. J. Radiat. Biol. Relat. Stud. Phys., Chem., Med.* **1982**, *42*, 449.

(27) Weaver, M. J.; Yee, E. L. *Inorg. Chem.* **1980**, *19*, 1936.

$k_{-1}[\mathrm{Ru}^{3+}] > k_2[\mathrm{H}^+]^2$, the constant k_1k_2/k_{-1}, and hence k_{-1}/k_2, can be determined. Since $K = k_1/k_{-1}$, we calculate $k_{-1} = 2.6 \times 10^5$ $\mathrm{M^{-1}\ s^{-1}}$. With $k_{-1}/k_2 = 4.6 \times 10^{-3}$ M, then $k_2 = 5.6 \times 10^7$ $\mathrm{M^{-1}\ s^{-1}}$. This acid solvolysis k_2 is in the range of the 2×10^8 $\mathrm{M^{-2}\ s^{-1}}$ found from the Pd/C-produced $\mathrm{Mn^{II}}$–TPPS and is in better agreement with a k_2 of 4.5×10^7 $\mathrm{M^{-2}\ s^{-1}}$ found by Neta and Morehouse,[28] who generated $\mathrm{Mn^{II}}$–TPPS by pulse radiolysis of aqueous 10% isopropyl alcohol/$\mathrm{N_2O}$-saturated solutions of $\mathrm{Mn^{III}}$–TPPS.

The reduction potential of $\mathrm{Mn^{III/II}}$–TAP is –0.15 V vs. NHE,[29] and thus $K = 2.3 \times 10^{-4}$ for the $\mathrm{Ru(NH_3)_6}^{2+}/\mathrm{Mn^{III}}$–TAP reaction. Since $k_1 = 33$ $\mathrm{M^{-1}\ s^{-1}}$, $k_{-1} = 1.4 \times 10^5$ $\mathrm{M^{-1}\ s^{-1}}$, and with $k_{-1}/k_2 = 5.5 \times 10^3$ M, $k_2 = 2.5 \times 10^7$ $\mathrm{M^{-2}\ s^{-1}}$. This acid solvolysis k_2 for the formally tetrapositive $\mathrm{Mn^{III}}$–TAP at $I = 0.3$ is similar to that of the formally tetranegative $\mathrm{Mn^{III}}$–TPPS. This is expected in that, at $I = 0.5$, zinc porphyrin acid solvolysis reactions of the oppositely charged Zn–$\mathrm{TAP^{4+}}$ and Zn–$\mathrm{TPPS^{4-}}$ complexes have approximately equal rates.[30] As the ionic strength decreases, however, the Zn–$\mathrm{TPPS^{4-}/H^+}$ solvolysis rates become much faster than those of Zn–$\mathrm{TAP^{4+}/H^+}$, in line with the Brønsted–Bjerrum equation.

The Marcus equation[31] can be used to calculate the self-exchange rate constants, k_{22}, for the $\mathrm{Mn^{III/II}}$–porphyrin studied. Taking the $\mathrm{Ru(NH_3)_6}^{2+/3+}$ self-exchange rate contant (k_{11}) as 3×10^3 $\mathrm{M^{-1}\ s^{-1}}$ (25 °C, $I = 0.1$),[27] we calculate $k_{22} = 3.2 \times 10^3$ $\mathrm{M^{-1}\ s^{-1}}$ for $\mathrm{Mn^{III/II}}$–TPPS and 2.6×10^3 $\mathrm{M^{-1}\ s^{-1}}$ for $\mathrm{Mn^{III/II}}$–TAP. A reduction potential of –0.010 V vs. NHE, which is independent of pH between 5 and 10, has been found[32] for $\mathrm{Mn^{III/II}}$–TMPyP(4), and the same number is assumed for the protonated manganese(III/II) tetrakis(4-pyridyl)porphyrin in acid.[33] An oxidation potential for the $\mathrm{V(H_2O)_6}^{2+/3+}$ couple of +0.230 V has been reported,[27] with a corresponding self-exchange rate constant $k_{22} = 1.5 \times 10^{-2}$ $\mathrm{M^{-1}\ s^{-1}}$. With use of an average value for k_{22} of 2.9×10^3 $\mathrm{M^{-1}\ s^{-1}}$ for a $\mathrm{Mn^{III/II}}$–porphyrin, the predicted cross reaction (k_{12}) rate constant for the presumed outer-sphere $\mathrm{V(H_2O)_6}^{2+}/\mathrm{Mn^{III}}$–TPyP(4) reaction is 390 $\mathrm{M^{-1}\ s^{-1}}$. This value is within a factor of 3 of the 145 $\mathrm{M^{-1}\ s^{-1}}$ observed earlier.[7] Thus, k_{22} appears to be relatively independent of the water-soluble manganese(III/II) porphyrin type, and similar conclusions have been reached for related cobalt(III/II) porphyrins.[34]

For the $\mathrm{Ru(NH_3)_6}^{2+}/\mathrm{Co^{III}}$–TMPyP(4) reaction, Pasternack and co-workers[13,14] found a k_{22} for $\mathrm{Co^{III/II}}$–TMPyP(4) of 20 $\mathrm{M^{-1}\ s^{-1}}$, close to the value of 21 $\mathrm{M^{-1}\ s^{-1}}$ for $\mathrm{Co(phen)_3}^{2+/3+}$. From the $\mathrm{Ru(NH_3)_6}^{2+}/\mathrm{Fe^{III}}$–TMPyP(4) reaction,[15] $k_{22} = 1.2 \times 10^6$ $\mathrm{M^{-1}\ s^{-1}}$ for high-spin $\mathrm{H_2O}$–$\mathrm{Fe^{III/II}}$–TMPyP(4), $>10^7$ $\mathrm{M^{-1}\ s^{-1}}$ for low-spin bis(imidazole)–$\mathrm{Fe^{III/II}}$–TMPyP(4), and $\geq 10^9$ $\mathrm{M^{-1}\ s^{-1}}$ for the low-spin HO–$\mathrm{Fe^{III/II}}$–TMPyP(4). The last two $\mathrm{Fe^{III/II}}$–porphyrin low-spin values were noted[15] to be in the range of 3×10^8 $\mathrm{M^{-1}\ s^{-1}}$ for $\mathrm{Fe(phen)_3}^{2+/3+}$, suggesting that electron transfer in low-spin porphyrin derivatives proceeds through the porphyrin π system.[36]

$k_{11} = 3 \times 10^{-4}$ $\mathrm{M^{-1}\ s^{-1}}$ for $\mathrm{Mn(H_2O)_6}^{2+/3+}$,[37] 7.7×10^{-5} $\mathrm{M^{-1}\ s^{-1}}$ for $\mathrm{Co(en)_3}^{2+/3+}$,[35] and 1.1 $\mathrm{M^{-1}\ s^{-1}}$ for[35] $\mathrm{Fe(H_2O)_6}^{2+/3+}$.[35] The ratios of the self-exchange rate constants for the $\mathrm{M^{III/II}}$ porphyrins to those of the saturated ligand complexes are 1×10^7 for manganese, 3×10^5 for cobalt, and 1×10^6 for iron. One thus sees an increase in exchange rates of ca. 10^6 when the metal ion moves from a hard environment into the soft porphyrin center.

Acknowledgment. This work was supported in part by Howard University NIH Biomedical Research Grant 5-SO-6-RR-08016-9 and PHS Grant No. GM-07799-05. We thank Dr. David Lavallee and Dr. P. Neta for helpful discussions.

Registry No. $\mathrm{Mn^{III}}$-TPPS, 88992-32-9; $\mathrm{Mn^{III}}$-TAP, 84177-73-1; $\mathrm{Ru(NH_3)_6}^{3+}$, 19052-44-9.

---

(28) Morehouse, K. M.; Neta, P. *J. Phys. Chem.* **1984**, *88*, 3118.

(29) Bettleheim, A.; Ozer, D.; Parasch, R. *J. Chem. Soc., Faraday Trans.* **1983**, *79*, 1555.

(30) Nwaeme, J.; Hambright, P. *Inorg. Chem.* **1984**, *23*, 1990.

(31) The Marcus equation[16] is of the form $k_{12} = (k_{11}k_{22}K_{12}f)^{1/2}$, where $\log f = (\log K_{12})^2/(4 \log (k_{11}k_{22}/10^{22}))$. k_{12} and K_{12} are the rate and equilibrium constants of the cross reaction, and k_{11} and k_{22} are the rate constants of the two self-exchange reactions.

(32) Harriman, A. *J. Chem. Soc., Dalton Trans.* **1984**, 141.

(33) For other limited pH range values of the $\mathrm{Mn^{III/II}}$–TMPyP(4) couple, see ref 26 and: Takahashi, K.; Komura, T.; Imanaga, H. *Bull. Chem. Soc. Jpn.* **1983**, *56*, 3203.

(34) Langley, R.; Hambright, P., manuscript in preparation.

(35) Brunschwig, B. S.; Creutz, C.; Macartney, D. H.; Sham, T.-K.; Sutin, N. *Faraday Discuss. Chem. Soc.* **1982**, *No. 74*, 113.

(36) Sutin, N. *Chem. Br.* **1965**, *4*, 2382.

(37) Diebler, H.; Sutin, N. *J. Phys. Chem.* **1964**, *68*, 174.

Contribution from the Departments of Chemistry,
Howard University, Washington, D.C. 20059,
and The American University, Washington, D.C. 20016

Deuterium-Substitution Effects on Relaxation Times and Interligand Nuclear Overhauser Effects for Assignment of Ligand Resonances and Isomer Identification in Cobalt(III) Complexes

C. B. Storm,* A. H. Turner, and N. S. Rowan

Received July 5, 1984

The assignment of proton resonances in heterocyclic ligands in coordination compounds is complicated by the variety of effects the metal ion can have on the ligand chemical shifts. Also, the assignment of closely related structural isomers by other than X-ray structure determinations is uncertain, at best. In this report we demonstrate the use of specific deuterium substitution effects on T_1's of ligand protons and interligand nuclear Overhauser effects (NOE) in making resonance and isomer assignments.

Proton resonances in nitrogen-containing heterocyclic ligands in metal complexes may be affected by a number of factors, including changes in electron density in the ligand due to σ-bond or d π-bond interactions, specific solvent–substrate interactions, changes in ligand magnetic anisotropy upon complex formation, paramagnetic anisotropy resulting from the temperature-independent paramagnetic moment of the metal ion, anisotropic effects of the metal–ligand bond, and ligand proton–metal ion nucleus spin–spin interactions. The likely relative importance of these different factors has been discussed by Foust and Ford.[1]

Imidazole complexes of $\mathrm{(NH_3)_5Co^{3+}}$($\mathrm{A_5Co^{3+}}$) have been studied as models for histidine complexes in biological systems,[2,3] and complexes of substituted imidazole have been prepared and characterized.[4] The assignment of resonances and isomers in these complexes is ambiguous, unless a specific isotopic substitution is made or an X-ray structure is available. We report here T_1 and NOE results for nine imidazole complexes and one histidine complex from which unequivocal resonance and isomer assignments can be made.

Experimental Section

^{1}H NMR spectra were obtained at 200.068 MHz on a Nicolet NT-200 spectrometer. T_1's were measured by using a standard inversion recovery sequence, 180–τ–90–acquire.[5] The T_1's were first estimated by obtaining a null point and τ values chosen to obtain an appropriate range of data points. The data were fit by a nonlinear least-squares program from the Nicolet 1180 software (DR-T_1-IR).

Nuclear Overhauser effects were obtained by comparing spectra with an F_2 frequency off-resonance to one with an ammine resonance of interest irradiated. Sufficient power was used to saturate the ammine resonance. The integrated areas of the peaks were compared or difference spectra obtained.

For NOE's and T_1's of protonated forms, the complexes were dissolved in 1 M DCl. Under this condition the N–H exchange is slow. For T_1's of deuterated forms, the complex was dissolved in $\mathrm{D_2O}$ and allowed to stand until all of the N–H had exchanged. Then, sufficient concentrated DCl was added to make the solution 1 M. No attempt was made to exclude air or to purify $\mathrm{D_2O}$ or other reagents.

Chemical shifts are reported on the δ scale relative to internal 3-(trimethylsilyl)propionate. T_1 values on duplicate measurements were reproducible to ±0.1 s.

---

* To whom correspondence should be addressed at Howard University.